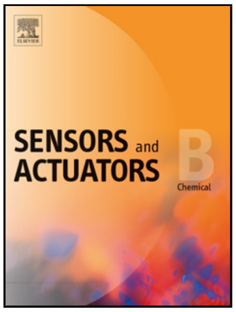

Title: ELECTROCHEMICAL SENSOR BASED ON MULTIWALLED CARBON NANOTUBE AND GOLD NANOPARTICLE MODIFIED ELECTRODE FOR THE SENSITIVE DETECTION OF BISPHENOL A

Authors: Najib Ben Messaoud, Mariana Emilia Ghica, Cherif Dridi, Mounir Ben Ali, Christopher M.A. Brett

PII: S0925-4005(17)31179-6
DOI: http://dx.doi.org/doi:10.1016/j.snb.2017.06.160
Reference: SNB 22631

To appear in: *Sensors and Actuators B*

Received date: 28-3-2017
Revised date: 9-6-2017
Accepted date: 23-6-2017

Please cite this article as: Najib Ben Messaoud, Mariana Emilia Ghica, Cherif Dridi, Mounir Ben Ali, Christopher M.A.Brett, ELECTROCHEMICAL SENSOR BASED ON MULTIWALLED CARBON NANOTUBE AND GOLD NANOPARTICLE MODIFIED ELECTRODE FOR THE SENSITIVE DETECTION OF BISPHENOL A, Sensors and Actuators B: Chemicalhttp://dx.doi.org/10.1016/j.snb.2017.06.160

ELECTROCHEMICAL SENSOR BASED ON MULTIWALLED CARBON NANOTUBE AND GOLD NANOPARTICLE MODIFIED ELECTRODE FOR THE SENSITIVE DETECTION OF BISPHENOL A

Najib Ben Messaoud[a,b], Mariana Emilia Ghica[c], Cherif Dridi[a],
Mounir Ben Ali[a,b], Christopher M.A. Brett[c,*]

[a] NANOMISENE Lab, LR16CRMN01, Centre for Research on Microelectronics and Nanotechnology CRMN of Technopark of Sousse B.P. 334, Sahloul, 4034, Sousse, Tunisia
[b] University of Sousse, ISSAT of Sousse, Cité Ettafala, 4003 Ibn Khaldoun Sousse, Tunisia
[c] Department of Chemistry, Faculty of Sciences and Technology, University of Coimbra, 3004-535 Coimbra, Portugal

*Corresponding author:
Tel: +351-239854470
Fax: +351-239827703
E-mail: cbrett@ci.uc.pt

Graphical abstract

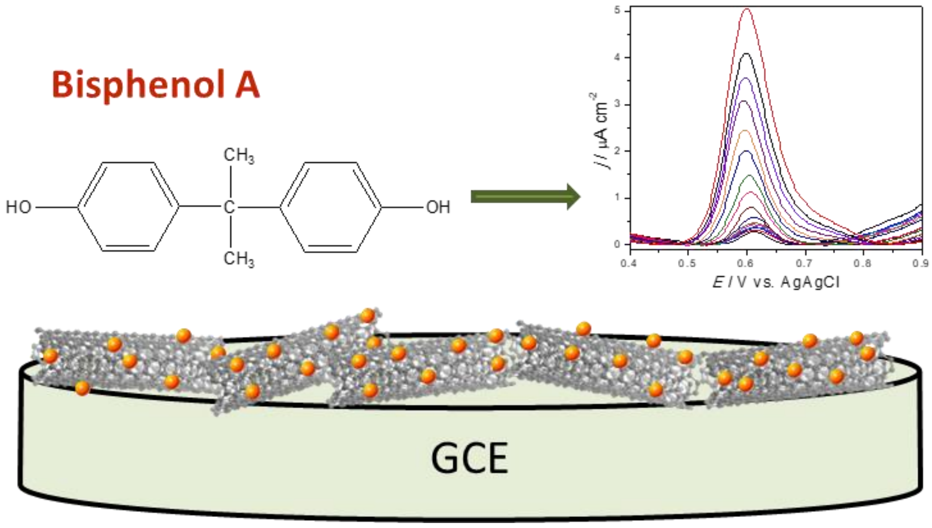

Highlights

- Bisphenol A electrochemical sensor using carbon nanotubes and gold nanoparticles
- Characterisation by voltammetry and electrochemical impedance spectroscopy
- Differential pulse voltammetry detection gives very low nanomolar detection limit
- Perspectives for impedimetric sensing assessed
- Application to analysis in waters

Abstract

A novel electrochemical sensor for bisphenol A comprising a multiwalled carbon nanotube (MWCNT) and gold nanoparticle (AuNP) composite modified glassy carbon electrode has been developed. Differential pulse voltammetric and electrochemical impedance characterisation were carried out. Modified electrode architectures with different MWCNT loadings and different numbers of deposited AuNP layers were tested, as well as the influence of pH. Under the best experimental conditions, the sensor exhibited a linear response to BPA from 0.01 μM to 0.7 μM, with a limit of detection of 4 nM, one of the lowest achieved up until now. The reproducibility, repeatability and stability of the sensor were examined and are superior to those reported in the literature using similar architectures for BPA sensors. Perspectives for an impedimetric sensor at micromolar concentrations were also assessed. Finally, the selectivity with respect to common interferents was demonstrated and practical application of the developed modified electrode for the determination of BPA in waters was successfully carried out.

Keywords: Bisphenol A; carbon nanotubes; gold nanoparticles; electrochemical sensor.

1. Introduction

With the development of the chemical industry, much industrial waste is being emitted into the environment, some of which has the potential to alter the structure and functions of the endocrine system and to be carcinogenic. Bisphenol A (BPA) is one of the key raw materials widely used in the production of epoxy resins and polycarbonate plastics [**1**], which have application in the chemical industry: metal food cans, bottles used as food and water containers, sports equipment, tableware and microwave ovenware [**2,3**]. Therefore, BPA will inevitably migrate into food and drinking water from product packaging, and thence humans may routinely ingest trace amounts of BPA.

BPA has attracted extensive attention due to its estrogenic activity [**4**], the probability of causing various kinds of cancer, including human prostate cancer the corresponding cells blocking testosterone synthesis, as well as exhibiting diverse pleiotropic actions in the brain and cardiovascular system [**5**]. BPA also exhibits an adverse effect on the human immune function, causing reproductive disorders including decrease of sperm quality in humans [**6**] resulting in neural and behavioural changes in infants and children [**7**]. Therefore, the development of new sensors for the detection of BPA at trace concentrations has become a very important subject of research. Different analytical methods have been developed and used for the determination of BPA including high-performance liquid chromatography [**8**], gas chromatography [**9**], enzyme-linked immunosorbent assay [**10**], molecular imprinting [**11**] and fluorimetry [**12**]. Electrochemical detection techniques have advantages in relation to these techniques of rapidity, low cost, high sensitivity, simple operation, good selectivity and real-time detection with in situ analysis **[13]**. Recently, electrochemical techniques have become very attractive methods for BPA detection **[14-17]**. Modification of the surfaces of such sensors with nanomaterials can enhance these advantages.

Carbon nanotubes (CNT) have excellent conductivity, chemical stability, large specific area, the ability to minimize surface fouling [**18**] and can accelerate the rates of electrochemical reactions [**19**]. There are many applications of carbon nanotubes, usually multiwalled carbon nanotubes (MWCNT), such as in batteries e.g. [**20**], nanoelectronic devices e.g. [**21**] and as nanomaterial modifiers of the surfaces of electrochemical sensors, e.g. [**22-26**].

Recently, attention has also been given to gold nanoparticles (AuNP) because of their good biological compatibility, high conductivity, high surface-to-volume ratio and catalytic/electrocatalytic properties. These properties of AuNP can be tuned by varying their size, shape, and the surrounding chemical environment. The analytical sensitivity of electrochemical sensors can be enhanced [**27,28**] and they can be a component of scaffolds for the fabrication of novel chemical and biological sensors [**29-32**].

Some of the materials which have been used for electrode modification for BPA determination are: molybdenum disulfide nanoflower-chitosan-Au nanoparticle composites [**33**], poly(amidoamine)-AuNP-silk fibroin [**34**], carbon nanotubes-β-cyclodextrin [**35**], and carboxylic group functionalized CNT-poly(3,4-ethylenedioxythiophene) [**1**].

In the present work, a novel electrochemical sensor for BPA detection consisting of a MWCNT plus AuNP modified glassy carbon electrode has been developed. There are two previous reports in the literature using MWCNT and AuNP together [**36,37**]; however, in [**36**] the sensor is based on paper as support and in both studies the electrode modification procedure is different from that developed here. Experimental parameters were optimized, including the pH of the buffer solution, and MWCNT and AuNP loading. The electrochemical behaviour of BPA was investigated by cyclic and differential pulse voltammetry and the analytical measurements were performed by differential pulse voltammetry and electrochemical impedance spectroscopy. Finally, the selectivity with respect to common interferents was demonstrated and practical application of the developed modified electrode for the determination of BPA was successfully carried out.

2. Experimental

2.1. Reagents and materials

Multi-walled carbon nanotubes (MWCNT) with ~95% purity, 30±10 nm diameter and 1-5 μm length were from NanoLab, U.S.A.

BPA was obtained from Sigma–Aldrich, Germany. A stock solution of 0.20 M BPA was prepared in methanol and stored in a refrigerator at 4 °C. Britton−Robinson (BR) buffer was used as supporting electrolyte, which contained a mixture of 0.040 M CH_3COOH, 0.040 M H_3PO_4 and 0.040 M H_3BO_3; the pH was adjusted between 4.0 and 9.0 by adding appropriate volumes of 2.0 M HCl or 5.0 M NaOH. All other chemicals were of analytical grade and used as received. Solutions were all prepared with Millipore Milli-Q nanopure water (resistivity ≥ 18 MΩ cm). All experiments were performed at room temperature (25 ± 1ºC).

2.2. Electrochemical measurements and instrumentation

A one-compartment 2 mL electrochemical cell contained a 1 mm diameter (geometric area 0.00785 cm^2) glassy carbon electrode (GCE) as working electrode, a platinum wire auxiliary electrode and Ag/AgCl (3M KCl) as reference.

Electrochemical voltammetric measurements were performed using a computer-controlled IviumStat potentiostat with IviumSoft software version 2.024 (Ivium Technologies, The Netherlands). In differential pulse voltammetry (DPV), pulse amplitude 50 mV, pulse time 100 ms, potential step 2 mV and scan rate 10 mVs^{-1} were used, unless otherwise indicated.

Measurements of pH were made with a CRISON 2001 micro pH-meter (Crison, Spain).

Electrochemical impedance spectroscopy (EIS) measurements were performed on a Solartron 1250 Frequency Response Analyser, coupled to a Solartron 1286 Electrochemical Interface (Solartron Analytical, UK) controlled by ZPlot 3.3a software (Scribner Associates Inc., USA).

The frequency range used was 65 kHz to 0.1 Hz, with 10 measurements per frequency decade and an rms perturbation voltage of 10 mV. Fitting of the spectra to equivalent circuits was done using ZView 2.,4 software (Scribner Associates Inc., USA).

2.3 Electrode preparation

The MWCNT were functionalized with carboxylate groups by nitric acid as previously reported [**22**]. The MWCNT dispersion of 0.05, 0.1, 0.2, 0.5 or 1.0 % was prepared by weighing 0.05, 0.1, 0.2, 0.5 or 1.0 mg and dispersing in 100 µL of 1.0 % chitosan solution dissolved in 1.0 % acetic acid. The prepared solution was then sonicated for 3 h.

For making gold nanoparticles, a volume of 200 mL of a solution of 0.01 % $HAuCl_4$ in water was prepared and brought to boiling point, then 7.0 mL of 1.0 % $Na_3C_6H_5O_7$ was slowly added under stirring [**38**] and left to react for 10 min. The solution was then left to cool to room temperature.

The bare glassy carbon electrode surface was polished with diamond spray (Kemet, UK) down to 1 µm particle size, rinsed thoroughly with ultra-pure water and dried in a flow of nitrogen gas before modification. To obtain the best response of the modified electrode, the amounts of AuNP and the concentration of MWCNT were optimized. The MWCNT (0.05, 0.1, 0.2, 0.5 or 1.0)/GCE was prepared by casting 2 µL of MWCNT (0.05, 0.1, 0.2, 0.5 or 1.0 %) dispersion on the surface of the cleaned GCE with a micropipette and drying at room temperature for 24 h. AuNP/GCE electrodes were obtained in a similar way by placing 2 µL of AuNP solution on the GCE surface. For fabricating AuNP/MWCNT/GCE, AuNP suspension was deposited on the surface of the previously prepared MWCNT/GCE. Different assemblies were prepared consisting of 3, 5 or 7 layers of AuNP on a MWCNT(0.2)/GCE, for each layer depositing 2 µL of AuNP suspension and drying under ambient conditions, resulting in AuNP(3)/MWCNT(0.2)/GCE, AuNP(5)/MWCNT(0.2)/GCE, and

AuNP(7)/MWCNT(0.2)/GCE, respectively. Additionally, AuNP(5)/MWCNT(0.05)/GCE and AuNP(5)/MWCNT(0.1)/GCE were prepared by depositing 5 layers of AuNP on MWCNT(0.05)/GCE and MWCNT(0.1)/GCE, respectively, these being used only for DPV analytical determination.

3. Results and discussion

3.1. Characterization of the modified electrodes

Unmodified and modified electrodes were characterized by differential pulse voltammetry (DPV) and electrochemical impedance spectroscopy (EIS) in the presence of BPA.

Figure 1 shows DPVs in BR buffer (pH=6) with 5.0 μM BPA at GCE, AuNP(5)/GCE, MWCNT(0.2)/GCE and AuNP(5)/MWCNT(0.2)/GCE. As expected, the oxidation peak current of BPA was lowest at the bare GCE. After modifying the electrode with AuNP, an increase of 40 % of the oxidation peak current was observed, which can be attributed to the greater accessible surface area on deposition of AuNP. At MWCNT(0.2)/GCE, the peak current increased much more, by 124 %, so that MWCNT led to a greater increase in active surface area than AuNP. With AuNP/MWCNT(0.2) on the surface of the GCE, the oxidation peak current increased even further, to 278 % of the value for an unmodified electrode. This can be attributed to the excellent high conductivity and large specific surface area of AuNP and MWCNT.

Electrochemical impedance spectroscopy was used to investigate the interfacial characteristics of the modified electrode. This technique has recently received attention in the field of analytical sciences, since it can furnish complementary information about the reaction dynamics and the membrane/solution structure. **Figure 2a** presents complex plane spectra of the bare GCE, AuNP(5)/GCE, MWCNT(0.2)/GCE and AuNP(5)/MWCNT(0.2)/GCE in BR buffer (pH=6) containing 9.0 mM BPA. A small decrease in the impedance was observed when the GCE was modified with AuNP. However, with the addition of MWCNT a big decrease in this value occurred, indicating that their presence on the surface of GCE enhances the conductivity and facilitates electron transfer. With AuNP on top of MWCNT, a further decrease was obtained, showing there is a synergetic effect of these two nanomaterial modifiers, in agreement with the DPV results. The impedance values follow the order: GCE > AuNP(5)/GCE > MWCNT(0.2)/GCE > AuNP(5)/MWCNT(0.2)/GCE.

The spectra were fitted using two equivalent circuits. The first comprises the cell resistance, R_Ω, in series with a parallel combination of a charge transfer resistance, R_{ct}, and a constant phase element, CPE. The CPE is modelled as a non-ideal capacitor according to the relation CPE = $-1/(C\mathrm{i}\omega)^\alpha$, where C is the capacitance (describing charge separation at the double layer interface), ω is the angular frequency and α is the CPE exponent (due to non-uniformity and roughness of the surface and interfaces). This circuit was used for the spectra obtained at the non-modified and gold nanoparticle modified electrode, which present semicircle-like spectra. The capacitance represents charge separation within the modifier layer, especially at the AuNP/MWCNT interface, and CNT at the modified electrode/solution interface, its value increasing markedly with the presence of both, that can be attributed to the high surface area of the AuNP/MWCNT interface. For GCE modified with carbon nanotubes, without and with AuNP, the spectra exhibited a small linear angular part at higher frequencies, before the semicircle, that can represent diffusion within the modifier layer. For this reason a diffusion impedance element Z_D was added in series before the parallel combination, expressed by $Z_D = R_D\ \mathrm{cth}[(\tau i\omega)^\alpha](\tau i\omega)^{-\alpha}$, where $\alpha \leq 0.5$, τ is the diffusional time constant and R_D the diffusional resistance. Since the first circuit is a simplified version of the second one, only the latter is illustrated in **Figure 2b**.

The values obtained from the fitting circuit are shown in **Table 1**. The results show that with each modification there is a gradual increase in the capacitance values, denoting accumulation of charge at the electrode surface, which is accompanied by a decrease of charge transfer resistance, indicating easier electron exchange. The lowest charge transfer resistance was obtained at AuNP(5)/MWCNT(0.2)/GCE. This is in agreement with the differential pulse voltammetry results, where the highest response for BPA was obtained at the same modified electrodes.

3.2. Electrochemical behaviour of BPA at modified electrodes

The electrochemical behaviour of bisphenol A at the electrode which exhibited the best performance, AuNP(5)/MWCNT(0.2)/GCE, was investigated by cyclic voltammetry (CV) and differential pulse voltammetry (DPV).

The influence of scan rate on the oxidation of 10 μM BPA at AuNP(5)/MWCNT(0.2)/GCE was studied by CV and is illustrated in **Figure 3a**. It can be seen that peak current density, j, increases linearly with scan rate (v) in the range 10 to 100 mV s^{-1}, **Fig. 3b**, indicating that the electrochemical oxidation of BPA at the AuNP/MWCNT/GCE is an adsorption-controlled process. A plot of logarithm of peak current density versus logarithm of scan rate was linear with a slope of 0.95, **Fig. 3c**, almost equal to the theoretical value of 1.0 for an adsorption-controlled process. The same behaviour was observed also in [1,35,39-42]. Adsorption was verified by repeated cyclic voltammograms at 100 mV s^{-1}, exhibiting a decrease in the oxidation current peak with each scan: 87.8 % in the 2nd, 75.6 % in the 3rd and 55.6 % in the 4th scan. However, the adsorption was reversible since, after placing the electrode in clean buffer solution and then scanning, no peak appeared.

The effect of buffer pH on the electrochemical oxidation response of 10 μM BPA at the AuNP(5)/MWCNT(0.2)/GCE was studied by DPV in the pH range from 4.0 up to 9.0, **Figure**

4a. The peak potential, E_{pa}, shifted negatively with increase of pH following a linear relationship, **Figure 4b,** with a slope of 56 mV per unit of pH, close to the theoretical value of 59 mV for an equal number of electrons and protons involved in the electrode reaction. The peak width at half height, $W_{1/2}$, given by $W_{1/2} = 90/n$ mV **[43]** for a reversible reaction, was approximately 58 mV over a wide range of concentrations, showing that 2 electrons are involved. It can be concluded that the oxidation mechanism involves two electrons and two protons, which is in agreement with studies in the literature [1,35,37]. A possible oxidation mechanism of BPA at AuNP(5)/MWCNT(0.2)/GCE is proposed in Scheme 1 with formation of quinone, via an unstable intermediate. The peak current increases with increase of pH, up to pH 6.0, then decreases. Thus, pH 6.0 was selected as the optimum value in order to maximise the sensitivity for the determination of BPA.

3.3. Optimization of the modified electrode preparation and determination of bisphenol A

3.3.1. Differential pulse voltammetry

The objective of this work is to fabricate a highly sensitive electrochemical sensor for BPA detection. In order to achieve the best electrode configuration, different MWCNT and AuNP loadings were investigated for sensor preparation and the response to BPA was measured by DPV.

The effect of MWCNT loading was investigated by using the same volume (2 μL) of suspensions with three different concentrations of MWCNT cast on the GCE surface, these being 0.2, 0.5 and 1.0 %. When using 0.5 and 1.0 % MWCNT the background current was very noisy and the response to BPA was observed only at high concentrations; for this reason, these configurations were not considered for analytical determination of bisphenol. Hence, a loading of 0.2 % MWCNT was selected for further studies.

The effect of the amount of AuNP suspension cast onto the MWCNT(0.2)/GCE surface was also studied. As shown in **Table 2,** the lowest detection limit for BPA and the highest sensitivity was achieved using 5 layers of AuNP.

In order to understand better the role of MWCNT and AuNP and synergistic effects, two additional assemblies were prepared, both with 5 AuNP layers, but with lower loadings of MWCNT of 0.05 and 0.1 %. The results from the analytical determination of BPA at these last configurations are also included in Table 2. The conclusion was that AuNP(5)/MWCNT(0.2%)/GCE was the best for BPA measurement amongst the modified electrodes tested.

The electroanalytical determination of BPA using the optimized configuration, AuNP(5)/MWCNT(0.2%)/GCE, was performed by DPV and voltammograms obtained for different bisphenol concentrations are shown in **Fig. 5a**. The calibration plot constructed from the DPV response, illustrated in **Figure 5b**, clearly shows two linear segments, a behaviour which was also observed in other studies for BPA electroanalytical determination [**7, 39,40,44**]. This behaviour could be ascribed to the effects of the adsorption of BPA, which will increase the higher the BPA concentration and the change in slope could correspond to more than one layer. In fact, there is evidence from analysis of impedance spectra (see section 3.3.2 below) that the surface coverage with adsorbate becomes non-uniform at higher BPA concentrations.

The two linear regions at AuNP(5)/MWCNT(0.2%)/GCE were from 0.01 μM to 0.7 μM and from 0.7 μM to 7.0 μM following the equations j_{pa} (μM cm^{-2}) = 1.76c (μM) + 0.24 (R = 0.999) and j_{pa} (μM cm^{-2}) = 0.62c (μM) + 1.14 (R = 0.997), respectively. The detection limit calculated as (3xSD$_{blank}$)/slope was 4.3 nM (n=3). The limit of detection obtained by the proposed sensor is one of the lowest until now, as is clear from the comparison with previous reports at modified electrode sensors with similar architectures including nanomaterials, shown in **Table 3**. The sensor with lowest limit of detection in Table 3, 1.0 nM, contains reduced graphene oxide as well as MWCNT and AuNP [**49**], all of which increase the electroactive area of the modified electrode.

3.3.2. Electrochemical impedance spectroscopy

Electrochemical impedance spectroscopy (EIS) was previously used in BPA sensors [**39,40,42,47**], for modified electrode characterization in the presence of hexacyanoferrate species, and there are no reports on BPA detection by this technique. The impedimetric sensing properties of the AuNP(5)/MWCNT(0.2)/GCE towards BPA was therefore investigated. **Figure 6a** illustrates the complex plane impedance response in BR pH 6.0 and with different BPA concentrations. The equivalent electrical circuit used to fit the spectra is the one shown in **Figure 2b** and the data obtained from fitting are included in **Table 1**. The values of the capacitance are almost constant up to 0.9 mM BPA and then increase with increase in BPA concentration; the same behaviour was observed for the diffusional time and diffusional resistance. This could be due to more and more non-uniform adsorption at high concentrations of BPA; the values of the CPE exponent are smaller from 0.9 mM upwards. There is a gradual decrease in the charge transfer resistance value with increase in BPA concentration, described by a linear dependence of R_{ct} on the logarithm of BPA concentration over the range 10 µM to 1.6 mM, see **Figure 6b**, according to the equation R_{ct} (kΩ cm^2) = 1.51lg(c/mM) + 0.54. The reason for the logarithmic dependence is due to adsorption of the BPA on the electrode surface before oxidation takes place. The calculated limit of detection was 170 nM, which is about 40 times higher than that achieved by DPV, but the ability to distinguish the spectrum from that recorded without BPA means that in practice, it would be about 1 µM. It is therefore possible to quantify BPA by EIS, but only at higher concentrations.

3.4. Reproducibility, repeatability and stability at AuNP/MWCNT/GCE

Reproducibility, repeatability and stability are key elements of sensor performance. The relative standard deviation (RSD) for measuring 1.0 μM BPA by DPV at five different electrodes prepared in the same way was 1.1 %. This shows that the AuNP/MWCNT/GCE has very good reproducibility, higher than that achieved by the reports in [**36,39,42,47**]. The repeatability at the same electrode for BPA detection was also very high, with an RSD of 1.5 % for 5 repeated measurements, superior to other sensors [**36,47**]. The long-term stability of the developed sensor was investigated by keeping the electrode at room temperature for 4 weeks and measuring BPA twice per week. After this period, the sensor still maintained 85 % of its initial response, which indicates a good storage stability of the AuNP/MWCNT/GCE. The stability obtained by the present sensor is comparable with that in [**35,40,42,47**], except that in those studies the electrode was kept at 4 ºC.

3.5 Interferences and practical application

The selectivity of the electrochemical sensor towards BPA was investigated in the presence of some possible interfering substances at concentrations 100-fold higher than that of BPA, sufficiently high to ensure selectivity towards BPA. The interferents tested included: ethanol, hydroquinone, methanol, phenol, Ca^{2+}, K^{+}, Na^{+}, Mg^{2+} and Zn^{2+}; none of them exhibited a significant change in the BPA response, the signal change was less than 5 % for inorganic and less than 7 % for organic interferents, see results listed in **Table 4**. A 1000-fold higher concentration of calcium ions was also tested and the decrease in signal was 7.6 %.

A 100-fold higher concentration of inorganic cations has been also studied for other BPA sensors with less than 5 % [15,16,36] or 10 % interference [39]. Regarding organic interferences, the concentrations tested were between 20 and 100-fold higher than BPA [2,7,15,16,39,42] and for the 100-fold the interferences were less than 5 or 6 % [2,40]. In [39] for 30-fold higher interferences the response change was less than 10 %.

In natural samples, an excellent way to minimise effects from interferents, especially in complex matrices, is to use the standard addition method. In order to evaluate the performance of AuNP/MWCNT/GCE for practical analytical applications, the DPV procedure for the determination of BPA in real water samples was followed. Two water samples were used: one was river water collected from a local river and one was mineral water bought from a local market. One millilitre of each sample solution was added to 9 mL BR buffer (pH 6.0), which was then analysed by the standard addition method. No BPA was found in the water samples. The same samples were then spiked with different amounts of BPA, namely 30 and 50 nM, and the recoveries were in the range 95.2 % to 102.4 %, indicating that the sensor is perfectly adequate for application in natural samples.

4. Conclusions

A novel electrochemical sensor for bisphenol A based on a MWCNT and AuNP composite modified glassy carbon electrode has been developed. Different MWCNT loadings and amounts of AuNP were tested; among those tested, the best experimental conditions for detection limit and sensitivity were a 0.2 % dispersion of MWCNT in chitosan solution with deposition of 5 layers of AuNP. The AuNP/MWCNT/GCE modified electrodes show some clear advantages, such as a very low detection limit of 4 nM, good stability, repeatability and simple preparation process, with excellent selectivity. This is also the first report on BPA measurement by electrochemical impedance spectroscopy, at micromolar concentrations.

Acknowledgments

The authors gratefully acknowledge the financial support from the European Commission 7th Framework Programme Marie Curie Actions People IRSES N°294993 SMARTCANCERSENS and Fundação para a Ciência e a Tecnologia (FCT), Portugal projects

PTDC/QEQ-QAN/2201/2014, in the framework of Project 3599-PPCDT, and UID/EMS/00285/2013 (both co-financed by the European Community Fund FEDER). MEG thanks FCT for a postdoctoral fellowship SFRH/BPD/103103/2014.

References

[1] L. Zhang, Y.-P. Wen, Y.-Y. Yao, Z.-F. Wang, X.-M. Duan, J.-K. Xu, Electrochemical sensor based on f-SWCNT and carboxylic group functionalized PEDOT for the sensitive determination of bisphenol A, Chin. Chem. Lett. 25 (2014) 517–522.

[2] S. Poorahong, C. Thammakhet, P. Thavarungkul, W. Limbut, A. Numnuam, P. Kanatharana, Amperometric sensor for detection of bisphenol A using a pencil graphite electrode modified with polyaniline nanorods and multiwalled carbon nanotubes, Microchim. Acta 176 (2012) 91–99.

[3] K.V. Ragavan, N.K. Rastogi, M.S. Thakur, Sensors and biosensors for analysis of bisphenol-A, TrAC Trends Anal. Chem. 52 (2013) 248–260.

[4] A.V. Krishnan, P. Stathis, S.F. Permuth, L. Tokes, D. Feldman, Bisphenol-A: an estrogenic substance is released from polycarbonate flasks during autoclaving, Endocrinology 132 (1993) 2279–2286.

[5] R. Steinmetz, N.A. Mitchner, A. Grant, D.L. Allen, R.M. Bigsby, N. Ben-Jonathan, The xenoestrogen bisphenol A induces growth, differentiation, and c-fos gene expression in the female reproductive tract 1, Endocrinology 139 (1998) 2741–2747.

[6] E. Carlsen, A. Giwercman, N. Keiding, N.E. Skakkeb\a ek, Declining semen quality and increasing incidence of testicular cancer: Is there a common cause?, Environ. Health Perspect. 103 (1995) 137-139.

[7] Q. Wang, Y. Wang, S. Liu, L. Wang, F. Gao, F. Gao, W. Sun, Voltammetric detection of bisphenol a by a chitosan–graphene composite modified carbon ionic liquid electrode, Thin Solid Films 520 (2012) 4459–4464.

[8] Y. Ji, J. Yin, Z. Xu, C. Zhao, H. Huang, H. Zhang, C. Wang, Preparation of magnetic molecularly imprinted polymer for rapid determination of bisphenol A in environmental water and milk samples, Anal. Bioanal. Chem. 395 (2009) 1125–1133.

[9] E.M. Malone, C.T. Elliott, D.G. Kennedy, L. Regan, Rapid confirmatory method for the determination of sixteen synthetic growth promoters and bisphenol A in bovine milk using dispersive solid-phase extraction and liquid chromatography–tandem mass spectrometry, J. Chromatogr. B. 878 (2010) 1077–1084.

[10] B. De Meulenaer, K. Baert, H. Lanckriet, V. Van Hoed, A. Huyghebaert, Development of an enzyme-linked immunosorbent assay for bisphenol A using chicken immunoglobulins, J. Agric. Food Chem. 50 (2002) 5273–5282.

[11] W. Zhao, N. Sheng, R. Zhu, F. Wei, Z. Cai, M. Zhai, S. Du, Q. Hu, Preparation of dummy template imprinted polymers at surface of silica microparticles for the selective extraction of trace bisphenol A from water samples, J. Hazard. Mater. 179 (2010) 223–229.

[12] Y. Kim, J.B. Jeon, J.Y. Chang, CdSe quantum dot-encapsulated molecularly imprinted mesoporous silica particles for fluorescent sensing of bisphenol A, J. Mater. Chem. 22 (2012) 24075–24080.

[13] C.M.A. Brett, A.M. Oliveira-Brett, Electrochemical sensing in solution-origins, applications and future perspectives, J. Solid State Electrochem. 15 (2011) 1487-1494.

[14] T. Zhan, Y. Song, Z. Tan, W. Hou, Electrochemical bisphenol A sensor based on exfoliated Ni_2Al-layered double hydroxide nanosheets modified electrode, Sens. Actuators B Chem. 238 (2017) 962–971.

[15] H. Filik, A.A. Avan, Electrochemical determination of bisphenol A based on poly(chromotropic acid) modified glassy carbon electrode, Curr. Anal. Chem. 13 (2017) 1–10

[16] Y. Zhou, L. Yang, S. Li, Y. Dang, A novel electrochemical sensor for highly sensitive detection of bisphenol A based on the hydrothermal synthesized Na-doped WO_3 nanorods, Sens. Actuators B Chem. 245 (2017) 238–246

[17] B. Su, H. Shao, N. Li, X. Chen, Z. Cai, X. Chen, A sensitive bisphenol A voltammetric sensor relying on AuPd nanoparticles/graphene composites modified glassy carbon electrode, Talanta 166 (2017) 126–132

[18] P.M. Ajayan, Nanotubes from carbon, Chem. Rev. 99 (1999) 1787.

[19] P.J. Britto, K.S. Santhanam, A. Rubio, J.A. Alonso, P.M. Ajayan, Improved charge transfer at carbon nanotube electrodes, Adv. Mater. 11 (1999) 154–157.

[20] G. Che, B.B. Lakshmi, E.R. Fisher, C.R. Martin, Carbon nanotubule membranes for electrochemical energy storage and production, Nature 393 (1998) 346–349.

[21] S.J. Tans, A.R. Verschueren, C. Dekker, Room-temperature transistor based on a single carbon nanotube, Nature 393 (1998) 49–52.

[22] M.E. Ghica, C.M.A. Brett, Simple and efficient epinephrine sensor based on carbon nanotube modified carbon film electrodes, Anal. Lett. 46 (2013) 1379–1393.

[23] M.M. Barsan, M.E. Ghica, C.M.A. Brett, Electrochemical sensors and biosensors based on redox polymer/carbon nanotube modified electrodes: A review, Anal. Chim. Acta 881 (2015) 1–23.

[24] M.E. Ghica, G.M. Ferreira, C.M.A. Brett, Poly (thionine)-carbon nanotube modified carbon film electrodes and application to the simultaneous determination of acetaminophen and dipyrone, J. Solid State Electrochem. 19 (2015) 2869–2881.

[25] D. Kul, M.E. Ghica, R. Pauliukaite, C.M.A. Brett, A novel amperometric sensor for ascorbic acid based on poly (Nile blue A) and functionalised multi-walled carbon nanotube modified electrodes, Talanta 111 (2013) 76–84.

[26] M.E. Ghica, Y. Wintersteller, C.M.A. Brett, Poly (brilliant green)/carbon nanotube-modified carbon film electrodes and application as sensors, J. Solid State Electrochem. 17 (2013) 1571–1580.

[27] W. Hong, H. Bai, Y. Xu, Z. Yao, Z. Gu, G. Shi, Preparation of gold nanoparticle/graphene composites with controlled weight contents and their application in biosensors, J. Phys. Chem. C 114 (2010) 1822–1826.

[28] P. Kannan, S.A. John, Highly sensitive determination of hydroxylamine using fused gold nanoparticles immobilized on sol–gel film modified gold electrode, Anal. Chim. Acta 663 (2010) 158–164.

[29] V.K. Khanna, Nanoparticle-based sensors, Def. Sci. J. 58 (2008) 608.

[30] E. Boisselier, D. Astruc, Gold nanoparticles in nanomedicine: preparations, imaging, diagnostics, therapies and toxicity, Chem. Soc. Rev. 38 (2009) 1759–1782.

[31] U.H. Bunz, V.M. Rotello, Gold nanoparticle–fluorophore complexes: sensitive and discerning "noses" for biosystems sensing, Angew. Chem. Int. Ed. 49 (2010) 3268–3279.

[32] S. Zeng, K.-T. Yong, I. Roy, X.-Q. Dinh, X. Yu, F. Luan, A review on functionalized gold nanoparticles for biosensing applications, Plasmonics 6 (2011) 491–506.

[33] K.-J. Huang, Y.-J. Liu, Y.-M. Liu, L.-L. Wang, Molybdenum disulfide nanoflower-chitosan-Au nanoparticles composites based electrochemical sensing platform for bisphenol A determination, J. Hazard. Mater. 276 (2014) 207–215.

[34] H. Yin, Y. Zhou, S. Ai, R. Han, T. Tang, L. Zhu, Electrochemical behavior of bisphenol A at glassy carbon electrode modified with gold nanoparticles, silk fibroin, and PAMAM dendrimers, Microchim. Acta 170 (2010) 99–105.

[35] Y. Gao, Y. Cao, D. Yang, X. Luo, Y. Tang, H. Li, Sensitivity and selectivity determination of bisphenol A using SWCNT–CD conjugate modified glassy carbon electrode, J. Hazard. Mater. 199 (2012) 111–118.

[36] H. Li, W. Wang, Q. Lv, G. Xi, H. Bai, Disposable paper-based electrochemical sensor based on stacked gold nanoparticles supported carbon nanotubes for the determination of bisphenol A, Electrochem. Commun. 68 (2016) 104–107.

[37] X. Tu, L. Yan, X. Luo, S. Luo, Q. Xie, Electroanalysis of bisphenol A at multiwalled carbon nanotubes-gold nanoparticles modified glassy carbon electrode, Electroanalysis 21 (2009) 2491-2494.

[38] V. Shakila, K. Pandian, Preparation of gold nanoislands on various functionalized polymer-modified glass and ITO for electrochemical characterization of monolayer assembly of alkanethiols, J. Solid State Electrochem. 11 (2007) 296–302.

[39] Z. Zheng, Y. Du, Z. Wang, Q. Feng, C. Wang, Pt/graphene–CNTs nanocomposite based electrochemical sensors for the determination of endocrine disruptor bisphenol A in thermal printing papers, Analyst 138 (2013) 693–701.

[40] Y. Li, Y. Gao, Y. Cao, H. Li, Electrochemical sensor for bisphenol A determination based on MWCNT/melamine complex modified GCE, Sens. Actuators B Chem. 171 (2012) 726–733.

[41] Y. Lin, K. Liu, C. Liu, L. Yin, Q. Kang, L. Li, B. Li, Electrochemical sensing of bisphenol A based on polyglutamic acid/amino-functionalised carbon nanotubes nanocomposite, Electrochim. Acta 133 (2014) 492–500.

[42] J. Li, D. Kuang, Y. Feng, F. Zhang, M. Liu, Voltammetric determination of bisphenol A in food package by a glassy carbon electrode modified with carboxylated multi-walled carbon nanotubes, Microchim. Acta 172 (2011) 379–386.

[43] C.M.A. Brett, A.M. Oliveira Brett, Electrochemistry, principles, methods and applications, Oxford Science Publications, 1993.

[44] C. Hou, W. Tang, C. Zhang, Y. Wang, N. Zhu, A novel and sensitive electrochemical sensor for bisphenol A determination based on carbon black supporting ferroferric oxide nanoparticles, Electrochim. Acta 144 (2014) 324–331.

[45] W. Wang, X. Yang, Y.-X. Gu, C.-F. Ding, J. Wan, Preparation and properties of bisphenol A sensor based on multiwalled carbon nanotubes/$Li_4Ti_5O_{12}$-modified electrode, Ionics 21 (2015) 885–893.

[46] M. Najafi, M.A. Khalilzadeh, H. Karimi-Maleh, A new strategy for determination of bisphenol A in the presence of Sudan I using a ZnO/CNTs/ionic liquid paste electrode in food samples, Food Chem. 158 (2014)125–131.

[47] X. Niu, W. Yang, G. Wang, J. Ren, H. Guo, J. Gao, A novel electrochemical sensor of bisphenol A based on stacked graphene nanofibers/gold nanoparticles composite modified glassy carbon electrode, Electrochim. Acta 98 (2013) 167–175.

[48] E.R. Santana, C.A. de Lima, J.V. Piovesan, A. Spinelli, An original ferroferric oxide and gold nanoparticles-modified glassy carbon electrode for the determination of bisphenol A, Sens. Actuators B Chem. 240 (2017) 487–496.

[49] H. Yu, X. Feng, X.-X. Chen, J.-L.Qiao, X.-L. Gao, N. Xu, L.-J. Gao, Electrochemical determination of bisphenol A on a glassy carbon electrode modified with gold nanoparticles loaded on reduced graphene oxide-multi walled carbon nanotubes composite, Chin. J. Anal. Chem. 45 (2017) 713-720.

[50] F. Pogacean, A.R. Biris, C. Socaci, M. Coros, L. Magerusan, M.-C. Rosu, M.D. Lazar, G. Borodi, S. Pruneanu, Graphene-bimetallic nanoparticle composites with enhanced electro-catalytic detection of bisphenol A, Nanotechnol. 27 (2016) 484001.

Biographies

Najib Ben Messaoud is PhD student at the NANOMISENE LR16CRMN01 (NANOmaterials, MIcrosystems for Health, Environment and Energy) Laboratory at the Centre of Research on Microelectronics and Nanotechnology CRMN Technopark of Sousse. His research interests focus on the development and characterization of biosensors and electrochemical sensors for cancer biomarker detection and water quality monitoring.

Mariana Emilia Ghica received her Ph. D. degree at University of Coimbra, Portugal, in 2007, where she is currently a Postdoctoral Researcher. Her research interests include the development and characterization of new nanostructured electrode architectures, methods for biomolecule immobilization for new electrochemical (bio)sensors and their application in the food, health, pharmaceutical and environmental areas. Other current interests comprise HPLC and electrochemical determination of antioxidants in natural samples for DNA aging protection, immunosensors, corrosion and its inhibition.

Cherif Dridi is a Full Professor and Director of the NANOMISENE LR16CRMN01 (NANOmaterials, MIcrosystems for Health, ENvironment and Energy) Laboratory at the Centre of Research on Microelectronics and Nanotechnology CRMN Technopark of Sousse and founder of the GREENS Team in ISSAT of Sousse, University of Sousse. He is working mainly on the development of advanced organic and hybrid nanomaterials and their based (bio)sensors, Microsystems, solar cells and optoelectronic devices. He received his MSc degree in physics and his DEA in materials and devices for electronics from the faculty of Sciences of Monastir in 1994-96 and his PhD degree in Physics (Relationship between structural and electronic properties in conjugated polymers) from Faculty of sciences of Tunis (FST) in 2003. In this period he conducted several works in Polymer and Biomaterials Laboratory, Quantum Physics Laboratory and Institut Charles Sadron (Lyon, Paris and Strasbourg, France respectively). He received his HDR (Nanomaterials for Environment and Solar Energy Harvesting) from FST in 2010. His research activity concerned the study of structural, optical and electrical properties of new hybrid nanomaterials from which devices for solar energy conversion, environment monitoring and health diagnosis has been developed particularly (chem./bio) sensors, photodiodes and solar cells. He was a principal investigator in 5 international projects funded by NATO (“Development of Bio/Chemical Sensors for Detection of Amines and Aldehydes in Fish Meat”), Tunisian-French cooperation PHC Utique (i)

“Nanomaterials for energy conversion and environment”, (ii) “Design, simulation and fabrication of embedded implantable Microsystems: Application for Health” and Tunisian-Algerian “Metallic Oxydes and Application for Photovoltaïcs”. He is an expert researcher in 2 projects funded by NATO SFP “Novel Electrochemical Nano-Sensors for Toxic Ions Detection” and FP7 EC CANCERNANOSENS. He has published/presented over 100 papers/communications in the above mentioned scientific research areas.

Mounir Ben Ali is a Full Professor at University of Sousse, High Institute of Applied Science and Technology of Sousse (ISSAT) working mainly in the field of Biosensors and Bioelectronics. He received his M.Sc. degree in Physical chemistry from the Faculty of Sciences (Monastir, Tunisia) in 1995 and his PhD degree in integrated electronic devices from Ecole Centrale de Lyon (Lyon, France) in 2000. Then he occupied a postdoctoral position focused on Nano-functionalisation of Nano devices at CEMES (Toulouse, France). He obtained a HDR in physics (Faculty of Sciences of Tunis) in 2007. He is now the Team Leader of the GREENS research group at ISSAT of Sousse & permanent Member of NANOmaterials and MIcrosystems for Health care, Environment monitoring and Energy NANOMISENE RD Laboratory in the Centre for Research on Microelectronics and Nanotechnology, Technopark of Sousse (LR16CRMN01- CRMN of Sousse) working mainly on the development of electrochemical sensors and biosensors, Microsystems and physical chemistry of nano-structured bio-membranes. He has extensive experience (>15 years) in mentoring and training researchers from undergraduate through to doctoral level. Prof. BEN ALI is part of worldwide renowned scientists as editorial member of several peer-reviewed scientific journals. He was a principal investigator in different international projects funded by NATO and French-Tunisian cooperation: NATO Linkage CLG980621 (2004-2006), CNRS/DGRSRT 18469 (2007-2009). He was a coordinator of Science For Peace NATO Project (2012-2016) and FP7 European Project CANCERNANOSENS (2012-2016). He has published/presented over 90 papers/communications in the area of chemical and biosensors devices, nanomaterials and their applications. His main current interests are: simulation and characterization of electrochemical micro/nano-structured (bio) chemical sensors.

Christopher Brett is a professor of chemistry at the University of Coimbra, Portugal. His research interests include new nanostructured electrode materials and modified electrode surfaces, electrochemical sensors and biosensors, electroactive polymers, corrosion and its inhibition, and applications of electrochemistry in the environmental, health, food and pharmaceutical areas. He was President of the International Society of Electrochemistry (ISE) in 2007-8. He is an elected member of the Bureau of the International Union of Pure and Applied Chemistry (IUPAC) for the period 2012-19 and a member of the IUPAC Executive Committee 2016-17. He was President of the Physical and Biophysical Chemistry Division of IUPAC in 2006-7, is a former Chairman of the IUPAC Electrochemistry Commission, and was President of the Analytical Division of the Portuguese Chemical Society (2003-5). He is a Fellow of the Royal Society of Chemistry. He is also Director of the Electroanalysis and Corrosion Laboratory, Instituto Pedro Nunes, Coimbra, the technological innovation link between the University of Coimbra and the industrial sector. His research activity is documented by more than 280 papers and 20 chapters in multi-author books, and has been presented in many conferences and invited lectures. He is co-author of 2 undergraduate/graduate textbooks "*Electrochemistry. Principles, methods and applications*", 1993, and “*Electroanalysis*”, 1998, both Oxford University Press.

Figure captions

Figure 1 DPV of 5.0 μM BPA in BR buffer (pH=6) at different modified electrodes and at GCE.

Figure 2. (a) Complex plane impedance plots at different electrodes in BR buffer (pH=6) containing 9.0 mM BPA; inset is the magnified plot of AuNP(5)/MWCNT(0.2)/GCE. Lines show equivalent circuit fitting. (b) Equivalent electrical circuit used to fit the spectra.

Figure. 3. (a) Cyclic voltammograms at AuNP(5)/MWCNT(0.2)/GCE in BR buffer (pH=6) containing 10 μM BPA at various scan rates: 10, 20, 40, 60, 80 and 100 mV s^{-1}; **(b)** Plot of oxidation peak current density, j_{pa}, vs. scan rate; (c) Plot of log of peak current density vs. log scan rate.

Figure 4. (a) DPV of 10 μM BPA at AuNP(5)/MWCNT(0.2)/GCE in BR buffer with different pH values: 4, 5, 6, 7, 8, 9; **(b)** Variation of peak potential and peak current with pH.

Figure 5. (a) DPV recorded at AuNP(5)/MWCNT(0.2)/GCE for increasing concentrations of BPA in BR buffer (pH=6); **(b)** Corresponding calibration plot.

Figure 6. (a) Complex plane impedance spectra at AuNP(5)/MWCNT(0.2)/GCE for different BPA concentrations in BR buffer (pH=6) at 0.65V; **(b)** Variation of R_{ct} with log [BPA/mM]

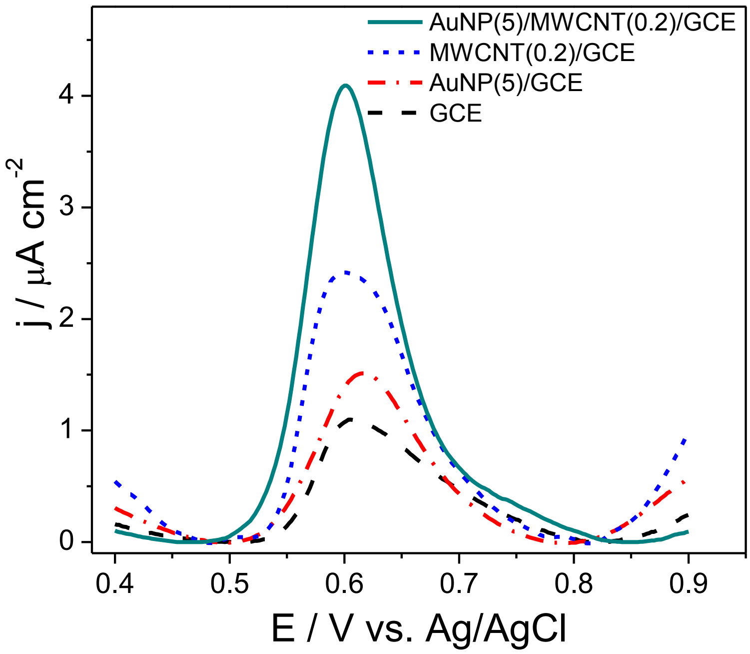

Figure 1. DPV of 5.0 μM BPA in BR buffer (pH=6) at different electrodes

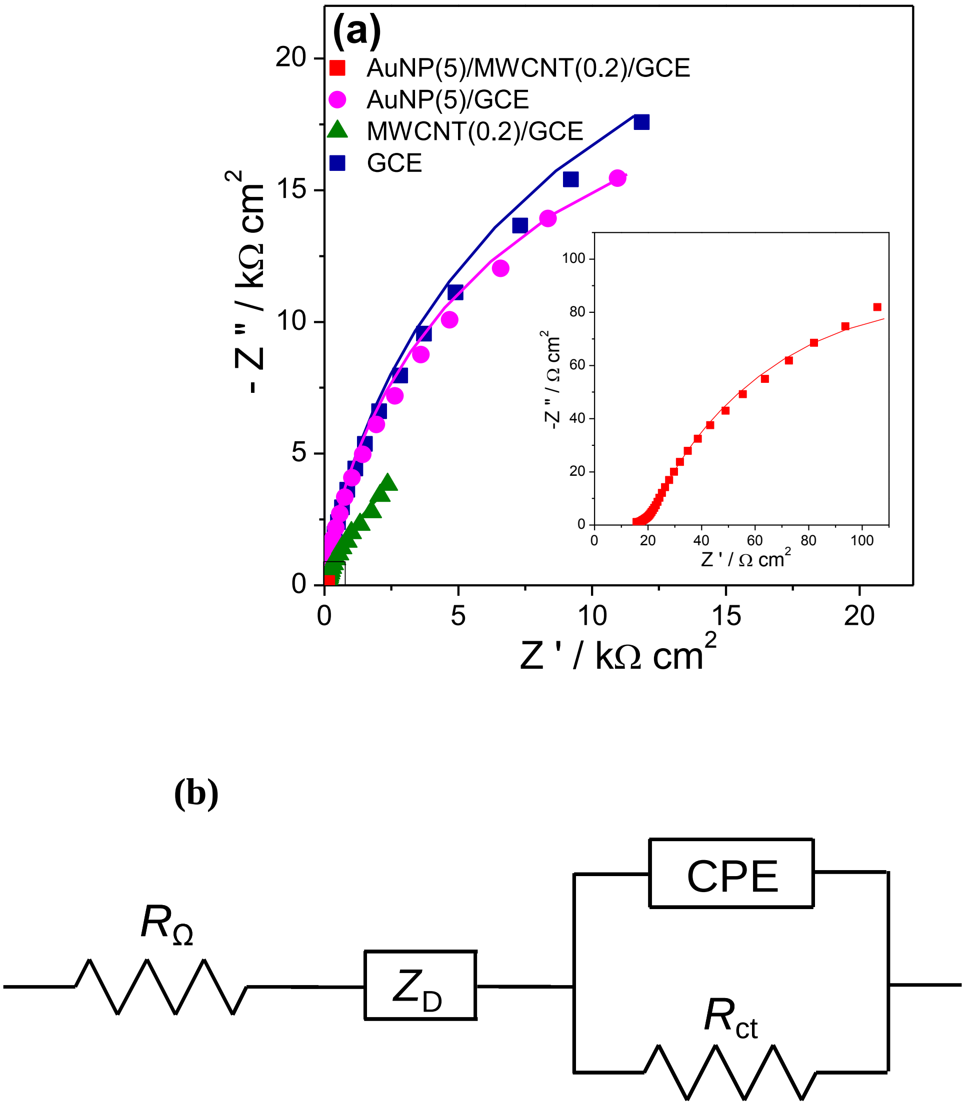

Figure 2. (a) Complex plane impedance plots at different electrodes in BR buffer (pH=6) containing 9.0 mM BPA; inset is the magnified plot of AuNP(5)/MWCNT(0.2)/GCE. Lines show equivalent circuit fitting. (b) Equivalent electrical circuit used to fit the spectra.

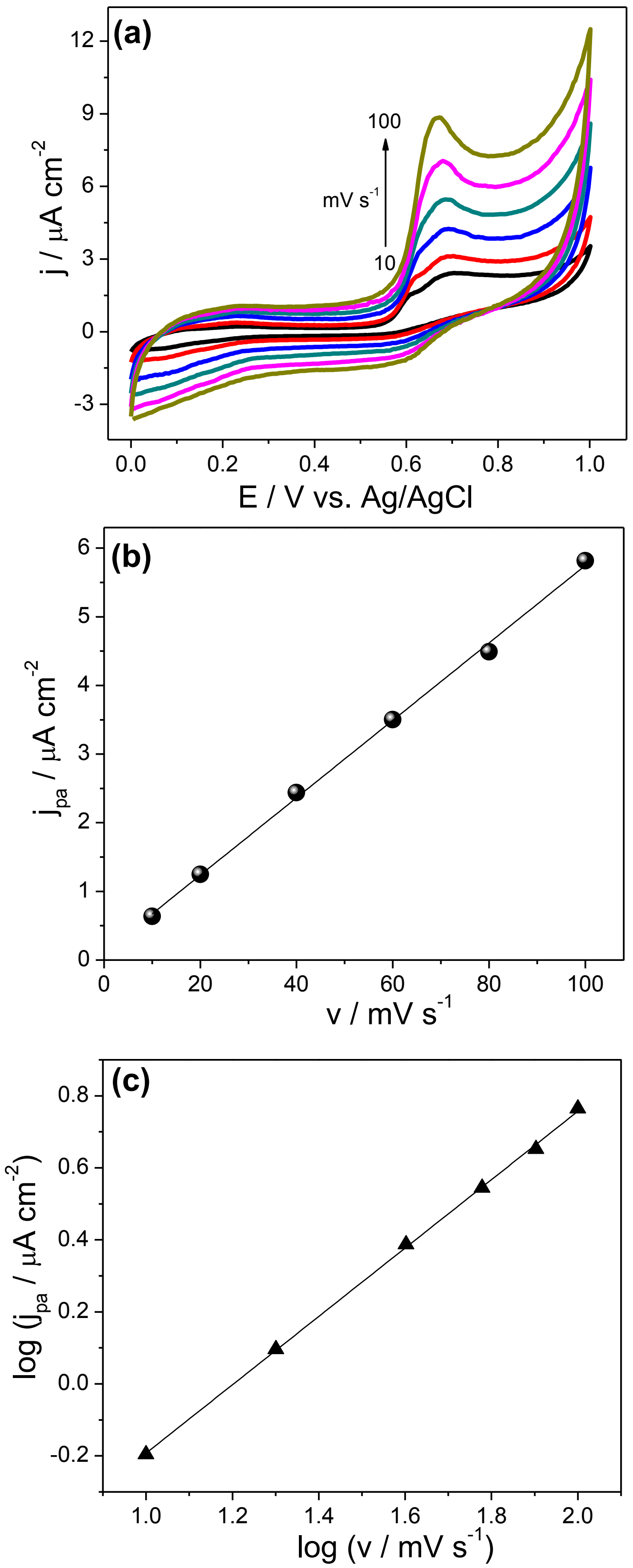

Figure 3. (a) Cyclic voltammograms at AuNP(5)/MWCNT(0.2)/GCE in BR buffer (pH=6) containing 10 μM BPA at 10, 20, 40, 60, 80 and 100 mV s^{-1}; **(b)** Plot of oxidation peak current density, j_{pa}, vs. scan rate; (c) Plot of log of peak current density vs. log scan rate.

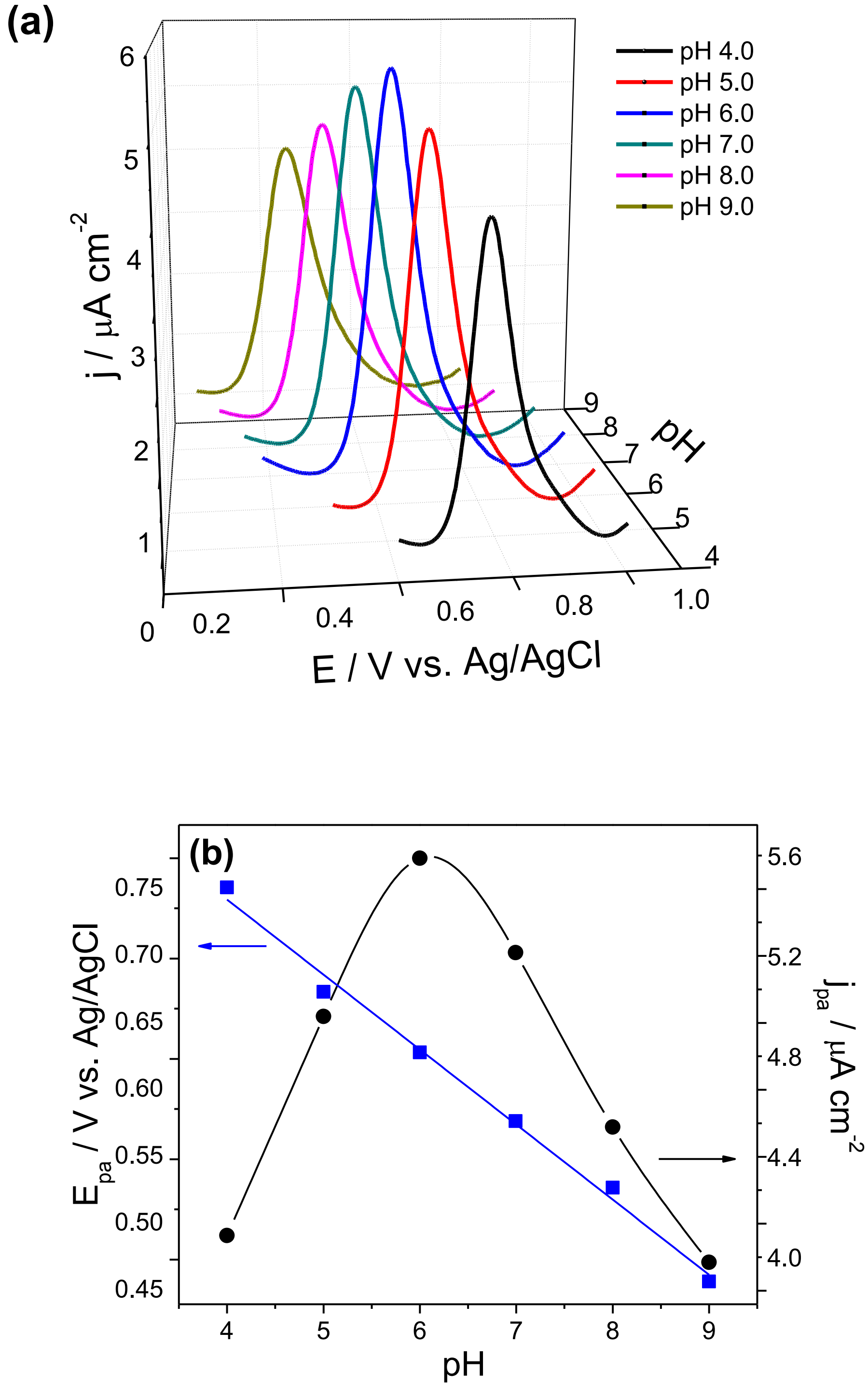

Figure 4. (a) DPV of 10 μM BPA at AuNP(5)/MWCNT(0.2)/GCE in BR buffer with different pH values: 4, 5, 6, 7, 8, 9; **(b)** Variation of peak potential and peak current with pH.

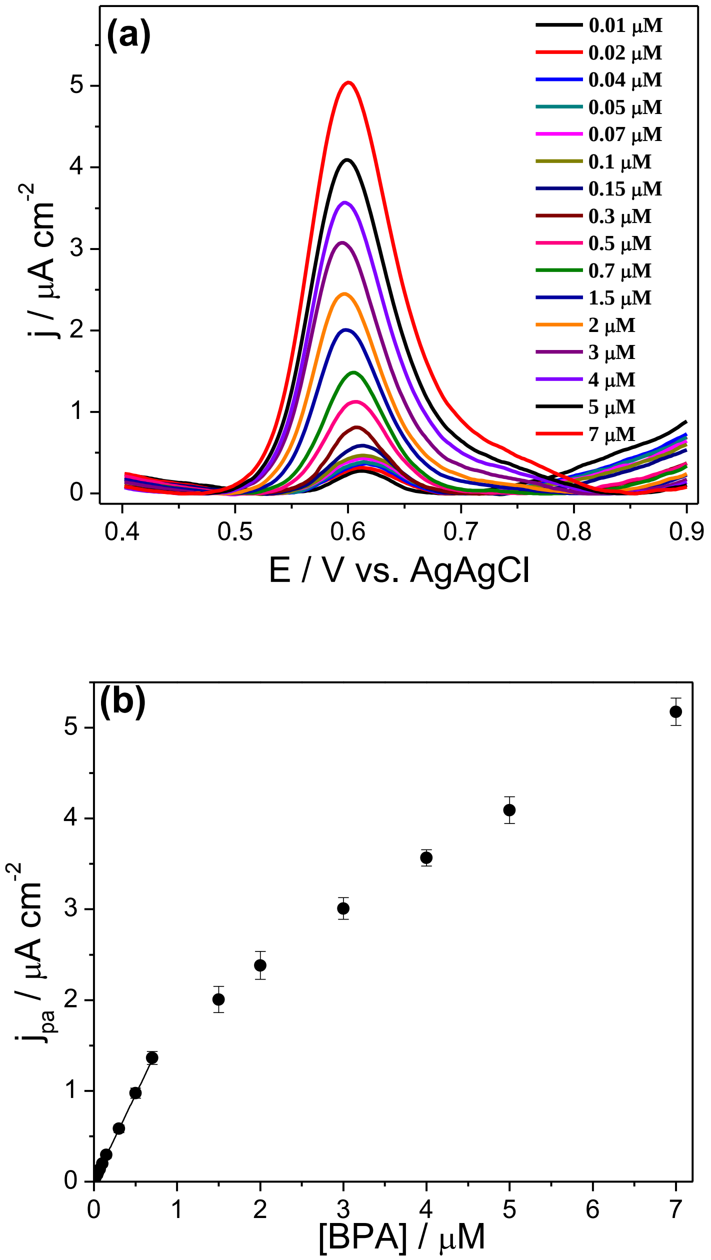

Figure 5. (a) DPV recorded at AuNP(5)/MWCNT(0.2)/GCE for increasing concentrations of BPA in BR buffer (pH=6); **(b)** Corresponding calibration plot

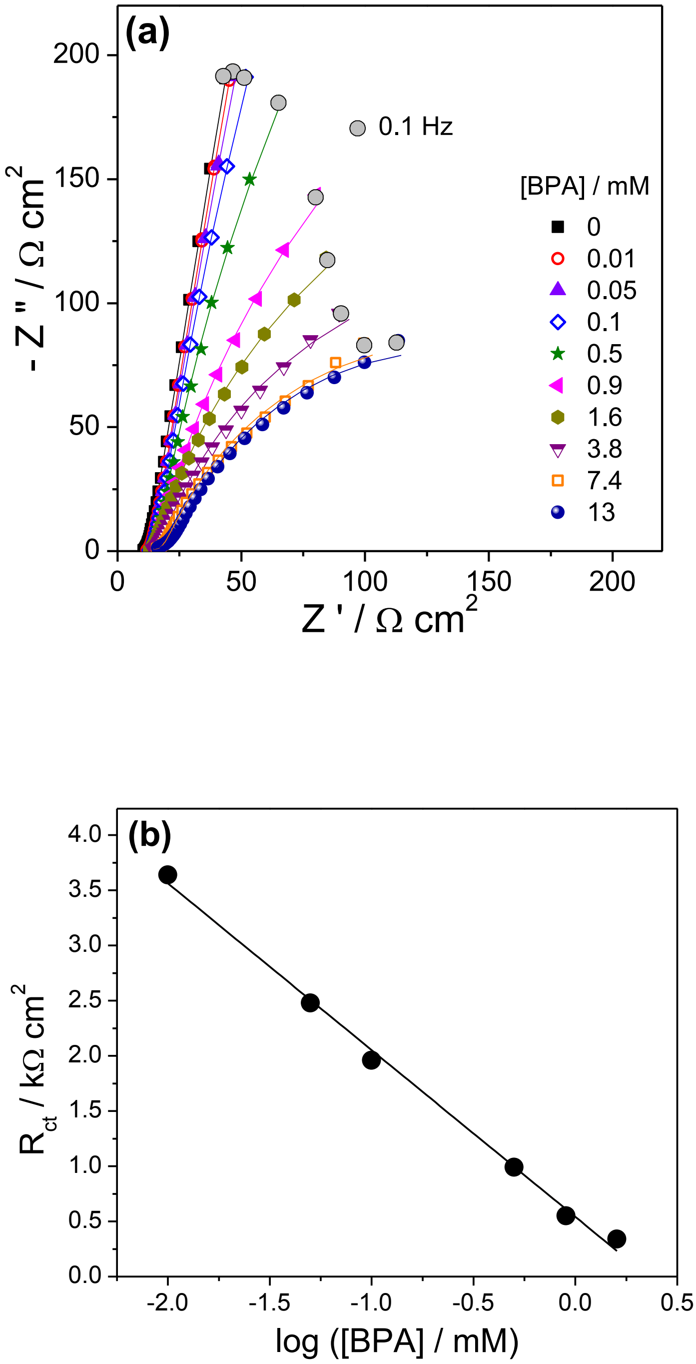

Figure 6. (a) Complex plane impedance spectra at AuNP(5)/MWCNT(0.2)/GCE for different BPA concentrations in BR buffer (pH=6) at 0.65V; **(b)** Variation of R_{ct} with log [BPA/mM]

Scheme 1. Possible oxidation mechanism of BPA at AuNP(5)/MWCNT(0.2)/GCE.

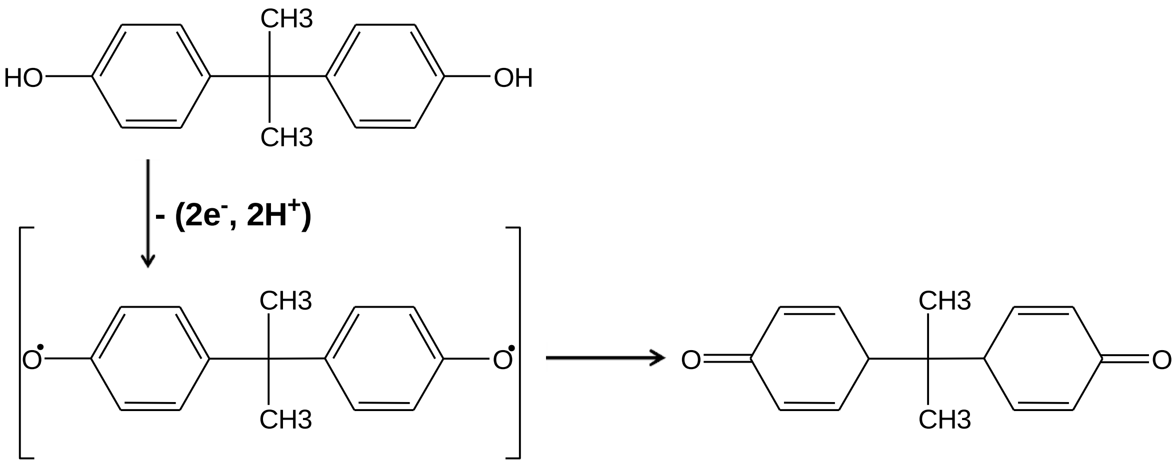

Scheme 1. Possible oxidation mechanism of BPA at AuNP(5)/MWCNT(0.2)/GCE

TABLES

Table 1. Experimental data obtained from fitting impedance spectra at different electrode configurations in the presence of 9.0 mM BPA and for different concentrations of BPA at AuNP(5)/MWCNT(0.2)/GCE

Electrode configuration (9.0 mM BPA)	R_Ω / Ω cm^2	Z_D / Ω cm^2 s$^{\alpha-1}$	τ / s	α	CPE / mF cm^{-2} s$^{\alpha-1}$	α	R_{ct} / kΩ cm^2
GCE	27	-	-	-	0.0021	0.92	57.5
AuNP(5)/GCE	26	-	-	-	0.0042	0.89	27.6
MWCNT(0.2)/GCE	35	120	0.23	0.30	0.282	0.94	4.9
AuNP(5)/MWCNT(0.2)/GCE	15	16.3	0.22	0.30	12.6	0.93	0.07
[BPA] / mM (AuNP(5)/MWCNT(0.2)/GCE)							
0	7	4.02	0.06	0.30	9.00	0.96	4.38
0.01	7	3.37	0.05	0.30	9.34	0.98	3.64
0.05	7	3.58	0.05	0.30	9.05	0.98	2.48
0.1	7	4.02	0.06	0.30	8.93	0.98	1.96
0.5	8	4.11	0.05	0.30	9.25	0.96	0.99
0.9	8	4.96	0.18	0.30	9.61	0.89	0.55
1.6	12	5.88	0.18	0.30	10.9	0.88	0.34
3.8	13	6.66	0.19	0.30	13.3	0.88	0.17
7.4	14	11.70	0.18	0.30	13.9	0.90	0.07

Table 2. Analytical parameters for BPA determination at different sensors; data from both linear ranges

Electrode configuration	Linear range / μM	Sensitivity / μA cm^{-2} $μM^{-1}$	Detection limit / nM
GCE	0.1-1.0/1.0-7.0	0.86/0.11	22.3
MWCNT(0.2%)/GCE	0.03-2.0/2.0-7.0	1.00/0.59	12.2
AuNP(3)/GCE	0.07-3.0/3.0-7.0	0.35/0.24	24.1
AuNP(3)/MWCNT(0.2%)/GCE	0.02-3.0/3.0-8.0	1.38/0.63	8.3
AuNP(5)/MWCNT(0.2%)/GCE	0.01-0.7/0.7-7.0	1.76/0.62	4.3
AuNP(7)/MWCNT(0.2%)/GCE	0.01-0.7/0.7-9.0	1.37/0.36	5.2
AuNP(5)/MWCNT(0.1%)/GCE	0.02-3.0/3.0-7.0	1.02/0.67	7.2
AuNP(5)/MWCNT(0.05%)/GCE	0.07-1.0/1.0-4.0	0.45/0.13	16.3

Table 3. Comparison of the analytical performance of the proposed sensor for BPA detection with other nanomaterial-modified electrode sensors from the literature

Electrode configuration	Method	Linear range / µM	Detection limit / nM	Ref.
SWCNT/PEDOT/GCE	CV	0.1-5.8	32	[1]
PANINR/MWCNT/PGE	Amp	1.0-400	10	[2]
Chit-Gr/CILE	DPV	0.1-100	26.4	[7]
AuPdNP/GrN/GCE	DPV	0.05-10.0	8.0	[17]
MWCNT/AuNP/Paper	LSV	0.876–87.6	131	[36]
AuNP/MWCNT/GCE	DPV	0.02–20.0	7.5	[37]
PtNP/GrO–MWCNT/GCE	DPV	0.06–10.0	42	[39]
MWCNT-MAM/GCE	Amp	0.01–10.8	5.0	[40]
PGA/MWCNT/GCE	DPV	0.1–10.0	20	[41]
MWCNT/GCE	LSV	0.01–10.0	5.0	[42]
$Li_4Ti_5O_{12}$/MWCNT/GCE	DPV	0.1–10.0	78	[45]
ZnO/MWCNT/CPE	SWV	0.002–700	9.0	[46]
AuNP/SGrNF/GCE	LSV	0.08–250	35	[47]
Fe_3O_4NPs-Si4Pic$^+$Cl$^-$/AuNPsSi4Pic$^+$Cl$^-$/GCE	DPV	0.02–1.40	7.0	[48]
AuNP/rGO-MWCNT/GCE	DPV	0.005-0.1	1.0	[49]
Gr-AuCuNP/AuE	LSV	0.1-30	1310	[50]
Gr-AgCuNP/AuE	LSV	0.1-100	1910	[50]
AuNP/MWCNT/GCE	DPV	0.01–0.7	4.3	This work

PEDOT-poly(ethylene dioxythiophene); PANINR – polyaniline nanorods; Chit-Chitosan; CILE – carbon ionic liquid electrode; PGE – pencil graphite electrode; AuPdNP – gold and palladium nanoparticles; PtNP - platinum nanoparticles; GrO - graphene oxide; rGrO-reduced graphene oxide; GrN-graphene nanosheets; MAM - melamine; PGA - polyglutamic acid; SGrNF - Stacked graphene nanofibers; LSV - linear sweep voltammetry; Amp - amperometry; SWV - square wave voltammetry

Table 4. Influence of interferents, concentration 100 μM, on the response to 1.0 μM BPA

Interferent	Peak change (%)
Ca^{2+}	-2.4
K^{+}	1.9
Na^{+}	-2.7
Mg^{2+}	-3.5
Zn^{2+}	3.1
Ethanol	-5.4
Hydroquinone	6.7
Methanol	-3.3
Phenol	3.0